Astronomy & Astrophysics manuscript no. main
December 16, 2021

R Coronae Borealis and dustless Hydrogen-deficient Carbon stars have different oxygen isotope ratios

V. Karambelkar[1,⋆], M. M. Kasliwal[1], P. Tisserand[2], G. C. Clayton[3], C. L.Crawford[3], S. G. Anand[1], T. R. Geballe[4] and E. Montiel[5]

[1] Cahill Center for Astrophysics, California Institute of Technology, Pasadena, CA 91125, USA
[2] Sorbonne Universites, UPMC Univ Paris 6 et CNRS, UMR 7095, Institut d'Astrophysique de Paris, IAP, F-75014 Paris, France
[3] Department of Physics & Astronomy, Louisiana State University, Baton Rouge, LA 70803, USA
[4] Gemini Observatory/NSF's NOIRLab, 670 N A'ohoku Pl, Hilo HI 96720, USA
[5] SOFIA-USRA, NASA Ames Research Center, MS 232-12, Moffett Field, CA 94035, USA

Received December 14, 2021;

ABSTRACT

Context. R Coronae Borealis (RCB) and dustless Hydrogen-deficient Carbon (dLHdC) stars are believed to be remnants of low mass white dwarf mergers. These supergiant stars have peculiar hydrogen-deficient carbon-rich chemistries and stark overabundances of ^{18}O. RCB stars undergo dust formation episodes resulting in large-amplitude photometric variations that are not seen in dLHdC stars. Recently, the sample of known dLHdC stars in the Milky Way has more than quintupled with the discovery of 27 new dLHdC stars.
Aims. It has been suggested that dLHdC stars have lower ^{16}O/^{18}O than RCB stars. We aim to compare the ^{16}O/^{18}O ratios for a large sample of dLHdC and RCB stars to conclusively examine this claim.
Methods. We present medium resolution (R≈ 3000) near-infrared spectra of 20 newly discovered dLHdC stars. We also present medium resolution (R≈ 3000 – 8000) *K*-band spectra for 47 RCB stars. We measure the ^{16}O/^{18}O ratios of 7 dLHdC and 31 RCB stars that show ^{12}C^{16}O and ^{12}C^{18}O absorption bands, and present the largest sample of values of ^{16}O/^{18}O for dLHdC and RCB stars to date.
Results. We find that six of the seven dLHdC stars have ^{16}O/^{18}O < 0.5, while 26 of the 31 RCB stars have ^{16}O/^{18}O > 1. We also confirm that unlike RCB stars, dLHdC stars do not show strong blueshifted (> 200 km s^{-1}) He I 10833 Å absorption, suggesting the absence of strong, dust-driven winds around them.
Conclusions. We conclude that most dLHdC stars have lower ^{16}O/^{18}O than most RCB stars. This confirms one of the first, long-suspected spectroscopic differences between RCB and dLHdC stars. Our results rule out the existing picture that RCB stars represent an evolved stage of dLHdC stars. Instead, we suggest that whether the white dwarf merger remnant is a dLHdC or RCB star depends on the mass ratios, masses and compositions of the merging white dwarfs.

Key words. Stars: late-type - carbon - AGB and post-AGB - supergiants - circumstellar matter - Infrared:stars

1. Introduction

R Coronae Borealis (RCB) and dustless Hydrogen-deficient Carbon (dLHdC) [1] stars are supergiants characterized by a peculiar chemical composition – an acute deficiency of hydrogen and an overabundance of carbon (Clayton 1996; Asplund et al. 2000). Together, they form the class of Hydrogen-deficient Carbon (HdC) stars. Their chemical compositions suggest that they are remnants of a He-core and a CO-core white dwarf (WD) merger (Webbink 1984; Clayton 2012), making them low mass counterparts of type Ia supernovae in the double-degenerate (DD) scenario (Fryer & Diehl 2008). In addition to peculiar chemical compositions, RCB stars experience rapid photometric declines (up to 8 mag in V band) that are attributed to dust formation episodes (Clayton 2012). dLHdC stars do not show any such declines or any significant infrared (IR) excess, suggesting that they do not undergo any dust formation (Clayton 2012). Why RCB stars produce dust while dLHdC stars do not, despite having no other known chemical differences is still a mystery.

It has been relatively easier to identify RCB stars than dLHdC stars owing to their spectacular photometric variations. There are 128 RCB stars known in the Milky Way, while only 5 Galactic dLHdC stars were known for the last four decades (Clayton 2012; Tisserand et al. 2020; Karambelkar et al. 2021). However, the sample of Galactic dLHdC stars has more than quintupled in the last year with the discovery of 27 new dLHdC stars (Tisserand et al. 2021, submitted). Additionally, several new RCB stars have been discovered and observed spectroscopically at near-infrared (NIR) wavelengths (Karambelkar et al. 2021).

NIR spectroscopic observations were key to identifying He-core and CO-core WD mergers as the progenitors of dLHdC and RCB stars. The K-band spectra of these stars show anomalously strong ^{12}C^{18}O first overtone bands in addition to the ^{12}C^{16}O first overtone bands (Clayton et al. 2005). The values of ^{16}O/^{18}O in dLHDC and RCB stars cover a remarkably wide range (from 0.3 to 50), thus in all cases 1–3 orders of magnitude smaller than the solar value (∼500). The large amount of ^{18}O is thought to be produced by partial helium burning in a thin shell around the core of the WD merger remnant, which is convectively dredged up to the surface (Clayton et al. 2007; Crawford et al. 2020).

⋆ viraj@astro.caltech.edu
[1] Historically, dLHdC stars were referred to as HdC stars. Here, we follow the updated nomenclature of Tisserand et al. 2021.

It has been suggested that in addition to dust production, $^{16}O/^{18}O$ ratios could be a second difference between RCB and dLHdC stars. Clayton et al. (2007) and García-Hernández et al. (2009) noted that dLHdC stars have $^{16}O/^{18}O < 1$ and most RCB stars have $^{16}O/^{18}O > 1$. However, this analysis is based on a small sample of only two dLHdC and five RCB stars [2]. Both dLHdC stars in the sample have $^{16}O/^{18}O < 1$, while three of the five RCB stars have $^{16}O/^{18}O > 1$. Karambelkar et al. (2021) measured the ratios for six additional RCB stars using medium resolution spectra and found that they had $^{16}O/^{18}O > 1$. However, additional measurements of these ratios for dLHdC stars were not possible in the past because of the five dLHdC stars known at the time, only three had temperatures cold enough to show the CO bands (García-Hernández et al. 2009, 2010; Karambelkar et al. 2021).

In this paper, we present the largest sample of $^{16}O/^{18}O$ values in dLHdC and RCB stars measured to date. We use medium resolution NIR spectra to measure $^{16}O/^{18}O$ for 7 dLHdC and 31 RCB stars. We also present *JHK*-band spectra of 21 (20 new, 1 previously known) dLHdC stars for the first time. Our results conclusively show that most dLHdC stars have lower $^{16}O/^{18}O$ than most RCB stars. In Section 2, we describe our spectroscopic observations, which include data collected over the last 15 years. In Section 3, we describe the NIR spectral features of dLHdC stars. We outline our methods for measuring $^{16}O/^{18}O$ in Section 4.1. We discuss the implications of the different oxygen isotope ratios for formation scenarios of RCB and dLHdC stars in Section 5, and conclude with a summary of our results in Section 6.

2. Data

Our data comprise medium resolution NIR spectra of 24 dLHdC stars and 47 RCB stars. The complete log of spectroscopic observations is presented in Table 1.

The spectra of 18 of the 20 newly discovered dLHdC stars were taken with the Triplespec spectrograph (Herter et al. 2008, R $\approx$ 3000) on the 200-inch Hale telescope at Palomar observatory on several nights between June and October 2021. Two newly discovered dLHdC star (A166 and A183) were observed with the SpeX spectrograph (R $\approx$ 2500) on the 3 m NASA Infrared Telescope Facility (IRTF, Rayner et al. 2003) on UT 20210623. We include a previously unpublished spectrum of the previously known dLHdC star HD 137613 taken with the UKIRT Imager Spectrometer (UIST, Ramsay Howat et al. 2004, R$\approx$3100) on the 3.8 m United Kingdom Infrared Telescope (UKIRT) on UT 20050309. We also include spectra of 3 other previously known dLHdC stars obtained with the Gemini Near-infrared Spectrograph (GNIRS, Elias et al. 2006) on the 8.1 m Gemini-South telescope in the long-slit mode with R $\approx$ 5900 in 2005, reported by Clayton et al. (2007).

The spectra of the RCB stars were collected over the last 15 years at three telescopes with four different instruments. We include spectra of 6 RCB stars obtained with Gemini South/GNIRS in September 2005 (Clayton et al. 2007). We include spectra of 2 more RCB stars observed with the Flamingos 2 spectrograph (Eikenberry et al. 2004) on the Gemini-South telescope in 2015. We observed the RCB star Z Umi with GNIRS on the Gemini-North telescope in 2011. In 2013, we observed 9 RCB stars with IRTF/SpeX at R $\approx$ 2500. We observed 12 more RCB stars in 2014 and 26 RCB stars in 2015 with IRTF/Spex at R $\approx$ 5000.

The Triplespec and IRTF spectra were reduced using the IDL package `spextool` (Cushing et al. 2004), and were flux calibrated and corrected for telluric absorption with standard star observations using `xtellcor` (Vacca et al. 2003). The UKIRT spectrum of HD 137613 was reduced in a standard manner using the Figaro software package for flatfielding, removal of the effects of cosmic ray hits, spectral and spatial rectification of the spectral images, wavelength calibration using an argon lamp, and ratioing by the spectrum of a standard star. The Gemini spectra were reduced similarly, but used a combination of IRAF and Figaro as described in Clayton et al. (2007).

3. NIR spectra of dLHdC stars

We present *JHK*-band NIR spectra of the 20 new dLHdC stars in Figure 1. We also include in the figure spectra of the previously known dLHdC star HD 137613 (green) and the RCB star NSV11154 (red, taken from Karambelkar et al. 2021).

The spectra of the dLHdC stars closely resemble NIR spectra of RCB stars taken at maximum light. The continuum shapes resemble those of F-G type stars. Numerous absorption lines are present. We identify strong absorption features attributed to C I (most prominently at 1.06883, 1.0686, 1.0688 and 1.06942 μm in the J-band and 1.73433, 1.74533 and 1.75104 μm in the H-band) and a blend of numerous Fe I, K I and Si I lines (see Rayner et al. (2003) for the wavelengths). H lines are absent in the NIR spectra of the dLHdC stars[3]. Only five of the twenty new dLHdC stars show $^{12}C^{16}O$ and $^{12}C^{18}O$ molecular features (presumably because the others are too hot for CO to exist in detectable amounts). Of the five, all but A166 also show the $^{12}C^{14}N$ bands at 1.0875, 1.0929, 1.0966, 1.0999 μm. Two additional stars B565 and A811 show CN but no CO bands.

3.1. Helium 1.0833 μm triplet

Our NIR spectra cover the He I 1.0833 μm triplet. This feature can serve as a tracer of high velocity winds around RCB and dLHdC stars. The levels of this transition are 20 eV above the ground state, and cannot be populated by photospheric radiation of dLHdC and RCB stars. Instead, they can be collisionally excited in high velocity winds around these stars. The He I feature has been observed in several RCB stars either as blueshifted absorption or with a P-Cygni profile with velocities as high as 500 km s^{-1} (Clayton et al. 2003, 2011; Karambelkar et al. 2021). The strength and velocity of the winds around RCB stars are greatest when the star has just emerged from a dust enshrouded minimum, and decrease with time thereafter. This suggests that the winds around RCB stars are dust-driven; i.e. the gas is dragged to high velocities by dust grains that are accelerated by radiation pressure. As dLHdC stars do not show dust excesses in their spectral energy distributions, we do not expect to see dust-driven winds around them. Geballe et al. (2009) observed the four previously known dLHdC stars and found no evidence for strong RCB-like He I absorption lines in their spectra.

Figure 2 shows a zoom-in of the NIR spectra of the new dLHdC stars around the He I 1.0833 μm triplet. We do not detect RCB-like (width > 200 km s^{-1}) helium absorption in the NIR spectra for any of the newly discovered dLHdC stars, except possibly A166. We cannot determine whether a lower velocity He I component is present from our medium resolution spectra, as we

[2] Note that the star HD 175893 was originally classified as a dLHdC star but is now known to be an RCB star based on an IR excess found by Tisserand (2012)

[3] See here for a list of NIR H lines

Table 1. Log of spectroscopic observations

Name	Class	Date	Tel./Inst.	Name	Class	Date	Tel./Inst.
HD 137613	dLHdC	09/03/2005	UKIRT/UIST	ASAS-RCB-17	RCB	08/2013,06/2015	IRTF/SpeX
HD 182040	dLHdC	09/2005	GS/GNIRS	ASAS-RCB-4	RCB	08/2013,06/2015	IRTF/SpeX
HD 148839	dLHdC	09/2005	GS/GNIRS	MACHO-401.48170.2237	RCB	08/2013,06/2015	IRTF/SpeX
HD 173409	dLHdC	09/2005	GS/GNIRS	ASAS-RCB-14	RCB	08/2013,08/2014	IRTF/SpeX
A183	dLHdC	23/06/2021	IRTF/SpeX	ASAS-RCB-18	RCB	08/2014	IRTF/SpeX
A166	dLHdC	23/06/2021	IRTF/SpeX	IRAS18135.5-2419	RCB	08/2014	IRTF/SpeX
C17	dLHdC	25/06/2021	P200/TSpec	EROS2-CG-RCB-4	RCB	08/2014	IRTF/SpeX
A223	dLHdC	25/06/2021	P200/TSpec	MACHO-308.38099.66	RCB	08/2014,06/2015	IRTF/SpeX
B42	dLHdC	25/06/2021	P200/TSpec	WISE_J194218.38-203247.5	RCB	08/2014	IRTF/SpeX
A226	dLHdC	25/06/2021	P200/TSpec	OGLE-GC-RCB-1	RCB	08/2014,06/2015	IRTF/SpeX
C38	dLHdC	29/06/2021	P200/TSpec	EROS2-CG-RCB-9	RCB	08/2014	IRTF/SpeX
C20	dLHdC	29/06/2021	P200/TSpec	EROS2-CG-RCB-11	RCB	08/2014	IRTF/SpeX
C105	dLHdC	02/07/2021	P200/TSpec	WISE_J183649.54-113420.7	RCB	08/2014	IRTF/SpeX
F75	dLHdC	02/07/2021	P200/TSpec	V739 Sgr	RCB	08/2014,06/2015	IRTF/SpeX
B565	dLHdC	15/09/2021	P200/TSpec	V3795 Sgr	RCB	08/2014	IRTF/SpeX
B566	dLHdC	15/09/2021	P200/TSpec	ASAS-RCB-5	RCB	06/2015	IRTF/SpeX
C528	dLHdC	15/09/2021	P200/TSpec	ASAS-RCB-7	RCB	06/2015	IRTF/SpeX
C539	dLHdC	15/09/2021	P200/TSpec	ASAS-RCB-16	RCB	06/2015	IRTF/SpeX
A811	dLHdC	15/09/2021	P200/TSpec	ASAS-RCB-19	RCB	06/2015	IRTF/SpeX
B567	dLHdC	15/09/2021	P200/TSpec	ASAS-RCB-20	RCB	06/2015	IRTF/SpeX
A798	dLHdC	15/10/2021	P200/TSpec	EROS2-CG-RCB-3	RCB	06/2015	IRTF/SpeX
C542	dLHdC	15/10/2021	P200/TSpec	EROS2-CG-RCB-10	RCB	06/2015	IRTF/SpeX
B563	dLHdC	15/10/2021	P200/TSpec	EROS2-CG-RCB-13	RCB	06/2015	IRTF/SpeX
A814	dLHdC	15/10/2021	P200/TSpec	FH Sct	RCB	06/2015	IRTF/SpeX
HD 175893	RCB	09/2005	GS/GNIRS	GU Sgr	RCB	06/2015	IRTF/SpeX
S Aps	RCB	09/2005	GS/GNIRS	RS Tel	RCB	06/2015	IRTF/SpeX
SV Sge	RCB	09/2005	GS/GNIRS	V482 Cyg	RCB	06/2015	IRTF/SpeX
ES Aql	RCB	09/2005	GS/GNIRS	V854 Cen	RCB	06/2015	IRTF/SpeX
WX CrA	RCB	09/2005	GS/GNIRS	V1783 Sgr	RCB	06/2015	IRTF/SpeX
U Aqr	RCB	09/2005	GS/GNIRS	V2552Sgr	RCB	06/2015	IRTF/SpeX
Z Umi	RCB	03/2011	GN/NIRI	VZ Sgr	RCB	06/2015	IRTF/SpeX
ASAS-RCB-11	RCB	08/2013	IRTF/SpeX	WISE_J174328.50-375029.0	RCB	06/2015	IRTF/SpeX
EROS2-CG-RCB-6	RCB	08/2013	IRTF/SpeX	V532 Oph	RCB	06/2015	IRTF/SpeX
V517 Oph	RCB	08/2013	IRTF/SpeX	HV 5637	RCB	11/2015	GS/F-2
V1157 Sgr	RCB	08/2013	IRTF/SpeX	EROS2-SMC-RCB-1	RCB	12/2015	GS/F-2
NSV 11154	RCB	08/2013	IRTF/SpeX				

cannot resolve possible contribution of He I to the Si I (1.0831 μm) line. A166 is the only dLHdC star that shows signs of an extended absorption component in addition to Si I absorption. If this is indeed the He I line, it would imply a wind velocity of ≈ 400 km s^{-1}. Higher resolution observations are necessary to identify the sources of this absorption.

Although we cannot completely resolve any possible low velocity He I component, our observations rule out the presence of strong, RCB-like dust-driven mass loss in dLHdC stars. This is expected, as none of these stars (except A166) shows a significant IR excess (Tisserand et al. 2021, submitted). We note, however, that this does not rule out the possibility that dLHdC stars were forming dust at some point in their history ($\gtrsim$ 10 years ago). Observations of XX Cam – an RCB star that has not entered a dust-enshrouded decline for the last six decades – do not show any significant He I features, similar to dLHdC stars (Geballe et al. 2009). The dust-driven He I wind is thus only a tracer of recent (few years to decades) dust-formation.

4. ^{16}O/^{18}O : Analysis and Results

4.1. Analysis

In this section we constrain the ^{16}O/^{18}O ratios of the five newly discovered dLHdC stars that show ^{12}C^{16}O and ^{12}C^{18}O bands, the previously known dLHdC stars HD 137613 and HD 182040 and 31 RCB stars that show the CO bands. Figure 3 shows the first four overtone CO bandheads of the seven dLHdC stars and six representative RCB stars. Even from visual inspection of the spectra, it is evident that in general the ^{12}C^{18}O absorptions are stronger in dLHdC stars than RCB stars. Here, we describe our procedure to derive constraints on the ^{16}O/^{18}O ratios from these and other spectra.

We follow the procedure described in Karambelkar et al. (2021). We first generate synthetic spectra using a grid of hydrogen-deficient spherically symmetric MARCS (Model Atmospheres in Radiative and Convective Scheme) atmospheric models with input compositions characteristic of RCB and dLHdC stars (log ϵ(H) = 7.5, C/He = 0.01, Gustafsson et al. 1975, 2008; Bell et al. 1976; Plez 2008). We generated the synthetic spectra using the package `TURBOSPECTRUM` (Alvarez & Plez 1998). We set log g = 1.0 and varied the effective temperatures

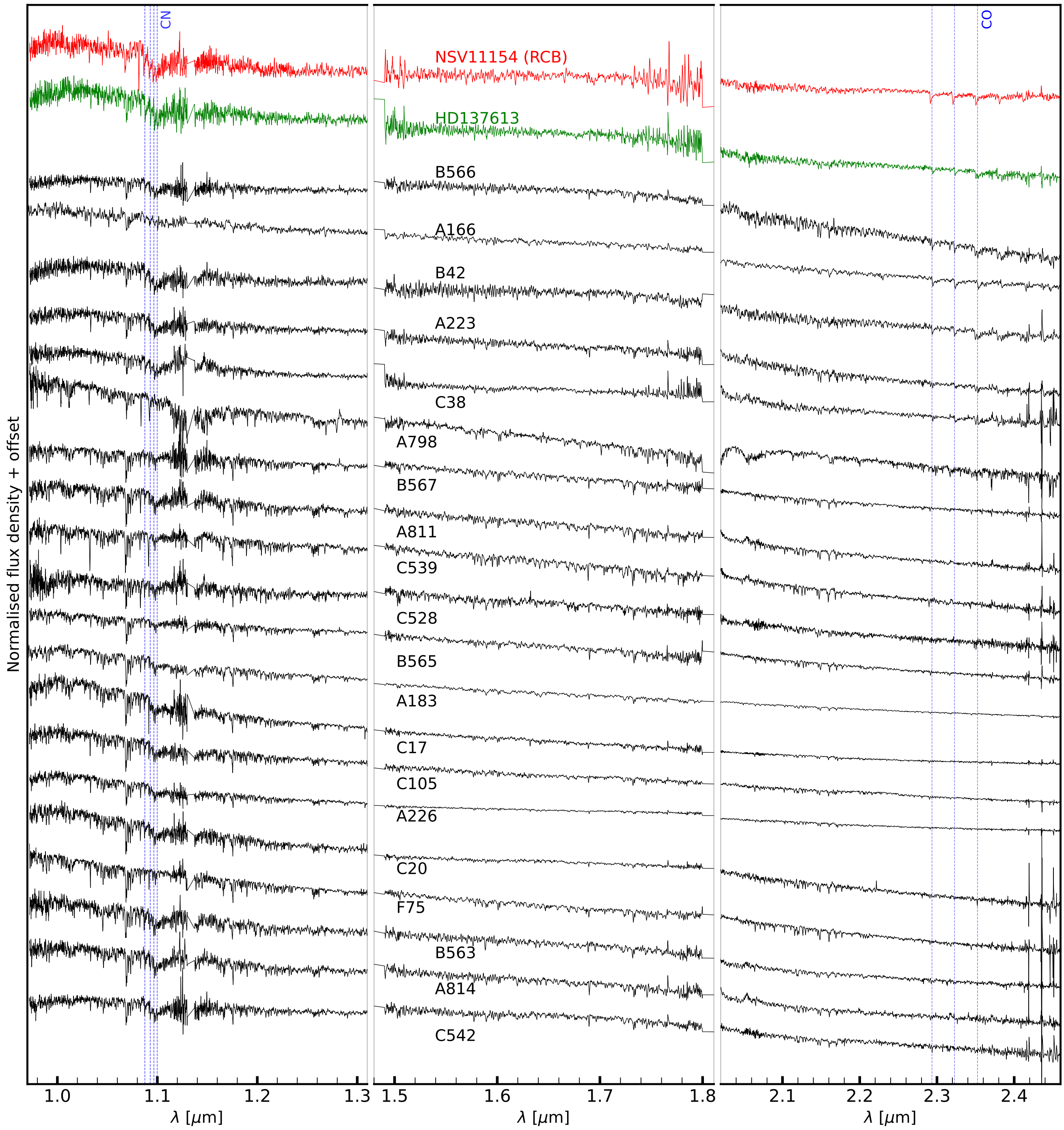

Fig. 1. NIR spectra of the newly discovered dLHdC stars. NIR spectra of the RCB star NSV11154 and the previously known dLHdC star HD137613 are also shown for comparison. The rest-frame positions of the CN and $^{12}C^{16}O$ absorption bands are indicated by dashed vertical lines.

from 4000 to 7500 K in intervals of 250 K. We chose $^{16}O/^{18}O$ values of 0.01, 0.05, 0.1, 0.2, 0.5, 1, 2, 5, 10, 20, 50, 500 and infinity (no ^{18}O). We used nitrogen abundances of log $\epsilon(N)$ = 7.0, 7.5, 8.0, 8.5 and 9.4. For RCB stars, the warm dust shell can contribute significantly to the K-band flux (up to 80%, Tisserand et al. 2013), filling up the absorption bands. To account for this, we introduced an additional parameter $f_{dust} = \frac{F_{shell,K}}{F_{total,K}}$, and varied it between 0 to 0.8 in steps of 0.1 for RCB stars. We do not expect this to be a significant effect for dLHdC stars as they do not have infrared dust excesses. We fit the synthetic spectra to continuum-normalised NIR spectra and visually examine each of the fits to determine the range of isotope ratios that is consistent with the observed spectra. The derived values of $^{16}O/^{18}O$ are listed in Table 2.

As noted in García-Hernández et al. (2009), it is challenging to measure the $^{16}O/^{18}O$ ratios accurately from medium resolution spectra. The $^{12}C^{16}O$ and $^{12}C^{18}O$ absorption bands can be contaminated by absorption from other molecules such as $^{12}C^{14}N$ and C_2. The absorption lines of CN and C_2 are densely packed in the K-band. It is also possible that the $^{12}C^{16}O$ absorption bands are saturated, resulting in a smaller measured $^{16}O/^{18}O$ ratios than the true value. There is also a degeneracy between the effects of the effective temperatures and nitrogen abundances on

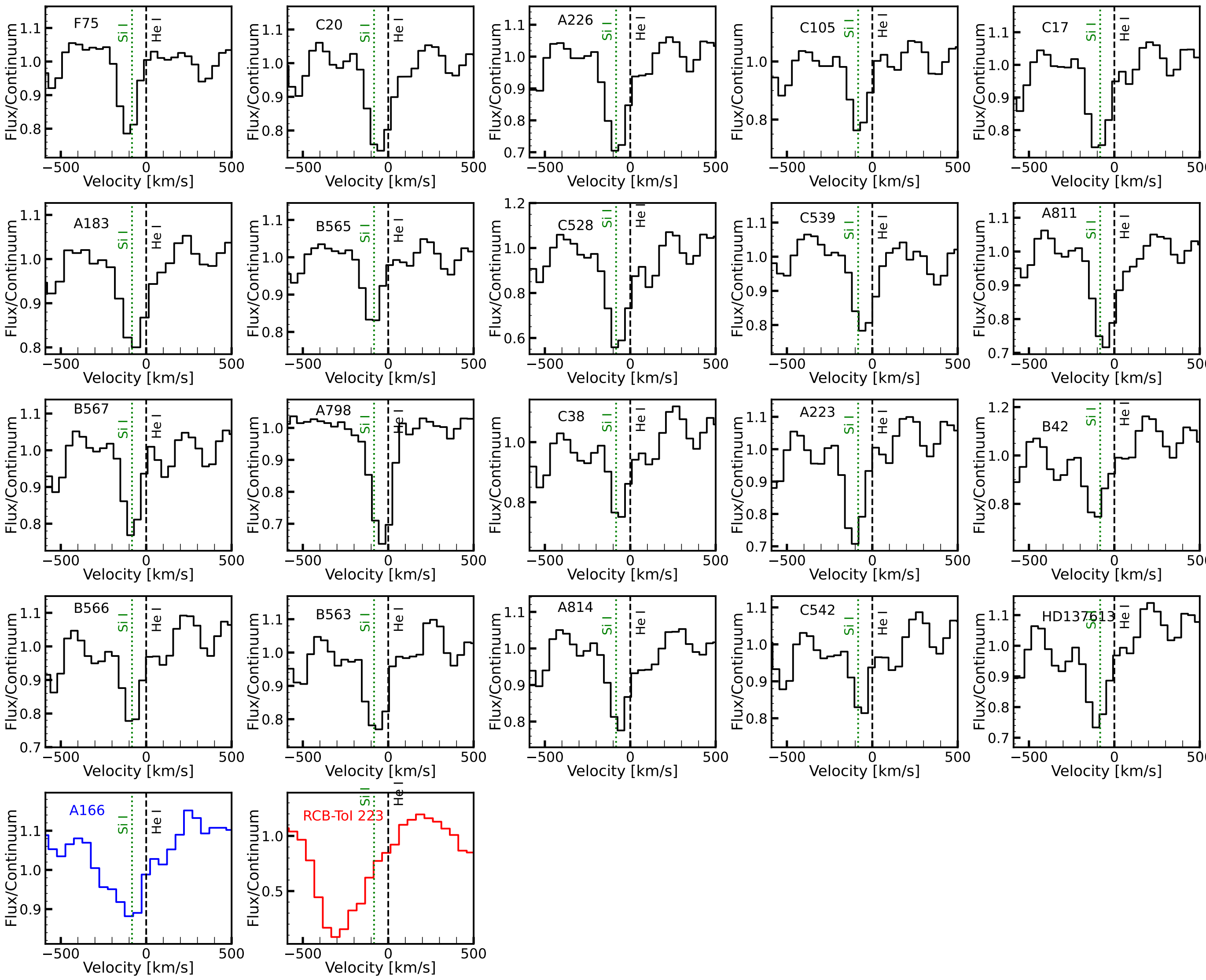

Fig. 2. Zoom in of the spectral region around the He I (10833 Å) triplet. The velocity is measured with respect to 1.0833 μm. The same spectral region of He I profile of an RCB star is shown in red – RCB-ToI-223 (a.k.a. WISE J182010.96-193453.4, at a phase when it has just emerged from a dust decline). We cannot resolve the contribution from the Si I line to any He I features from our low resolution spectra. However, it is evident that we do not detect any strong (> 200 km s^{-1}), RCB-like winds in any dLHdC star, suggesting that there is no dust-driven wind around them. This is consistent with no hot dust excess seen in the SEDs of any of these stars. A166 is the only dLHdC star that shows a possible high velocity He I absorption profile (blue).

the depths of the CO absorption bands. For these reasons, we are not able to tightly constrain ^{16}O/^{18}O, but instead provide a range of values combining the effects of the temperatures, nitrogen abundances and f_{dust}. Wherever possible, we use estimates of temperatures from the literature to tighten the constraints. Despite the wide range of ratios for each star, our measurements conclusively show that most dLHdC stars have a significantly lower ^{16}O/^{18}O than RCB stars.

4.2. Results

4.2.1. dLHdC stars

With the exception of A166, the depths of the ^{12}C^{18}O absorption bands in the dLHdC stars are comparable to those of the ^{12}C^{16}O bands (see Figure 3). From comparisons to synthetic spectra and using temperatures from Crawford et al. 2022 (in prep), we derive ^{16}O/^{18}O ratios in the ranges 0.05–0.2 for B42, C38 and B566, 0.1–0.5 for A223, HD 182040 and HD 137613. Our derived values for HD 137613 and HD 182040 are consistent with those reported by Clayton et al. (2007) from medium resolution and García-Hernández et al. (2009) from high resolution spectra.

For B42, none of the spectral models fit the CO features at 2.349 µm and 2.352 µm. This could be because the 2.352 µm ^{12}C^{16}O band is saturated. Fits to the 2.378 and 2.383 µm bands suggest ^{16}O/^{18}O = 0.05–0.2, but the only models that fit these bands have a low nitrogen abundance of log ϵ(N) = 7.0. The optical spectrum of B42 shows strong CN bands (see Tisserand et al. 2021), suggesting that the nitrogen abundance may not be so low. It is possible that the 2.383 µm ^{12}C^{16}O band in B42 is also saturated, and the value we report is lower than the true ^{16}O/^{18}O. If this is the case, our reported uncertainty on the ^{16}O/^{18}O of B42 is also likely underestimated, as it does not include the systematic uncertainty associated with the saturated bands and the nitrogen abundances. Higher resolution observations are necessary to measure the true nitrogen abundance and the true $^{16}O/^{18}O$ value of B42.

Unlike the other dLHdC stars, A166 shows significantly weaker $^{12}C^{18}O$ absorptions than the $^{12}C^{16}O$ absorption; we derive $^{16}O/^{18}O$ in the range of 20 – 500 for this star. Tisserand et al. 2021 note that A166 is an outlier among the newly discovered dLHdC stars. In the HR diagram, it is located near two cool RCB stars and is distant from most dLHdC stars. It also has IR excesses in the WISE W3 and W4 bands. This, together with its high, RCB-like value of $^{16}O/^{18}O$ and possible broad He I absorption suggests that it is an RCB star. However, the lack of IR excesses in the NIR, WISE W1 and W2 bands indicates that it is in a phase of low dust production, similar to XX Cam (see Section 4.6 of Tisserand et al. 2021).

4.2.2. RCB stars

Of the 31 RCB stars that show the CO overtone absorption bands, estimates of effective temperatures are available for 19 (Crawford et al. 2022, in prep). We are able to derive the tightest constraints on $^{16}O/^{18}O$ for them. For most of the remaining 12, we can only derive lower limits on $^{16}O/^{18}O$.

Most of the RCB stars in our sample have much weaker $^{12}C^{18}O$ absorption bands than dLHdC stars. Five of them have $^{16}O/^{18}O \gtrsim 500$ and thus do not show ^{18}O enrichment (compared to normal stars). A total of 26 of the 31 RCB stars have $^{16}O/^{18}O > 1$. Thus, a large majority of RCB stars have higher $^{16}O/^{18}O$ than dLHdC stars.

Five RCB stars – HD 175893, ASAS-RCB-11, IRAS 18135.5-2419, WX CrA and EROS2-CG-RCB-6 – have prominent $^{12}C^{18}O$ absorption features and are consistent with $^{16}O/^{18}O < 1$. We derive $^{16}O/^{18}O$ values of 0.01–0.2, 0.01–0.2, 0.5–5, 0.05–0.5 and 0.2–5 for these stars respectively. These values are similar to those of dLHdC stars. We note that our derived $^{16}O/^{18}O$ values for HD 175893, S Aps, SV Sge, ES Aql, U Aqr, Z Umi and WX Cra agree with previous medium resolution measurements from Clayton et al. (2007). Our derived values also agree with high resolution measurements for all of these except S Aps, SV Sge and ES Aql, as the $^{12}C^{16}O$ bandheads are saturated in these three (García-Hernández et al. 2010). Finally, the RCB star EROS2-CG-RCB-4 shows the $^{13}C^{16}O$ absorption bandhead at 2.345, 2.374, 2.404 and 2.434 μm (see Figure 3).

To summarize, we find that most dLHdC stars have $^{16}O/^{18}O <$ 1, lower than most RCB stars. However, there is an overlap – a small fraction of dLHdC stars have $^{16}O/^{18}O > 1$ while a small fraction of RCB stars have $^{16}O/^{18}O < 1$. We illustrate this in Figure 4.

5. Discussion

Our NIR spectroscopic observations have revealed that in addition to dust-formation, dLHdC and RCB stars can in most cases be distinguished based on their values of $^{16}O/^{18}O$. dLHdC stars in general have a lower $^{16}O/^{18}O$ than RCB stars. It is not surprising that the oxygen isotope ratios are an important factor in the study of dLHdC and RCB stars. Anomalously low $^{16}O/^{18}O$ in dLHdC and RCB stars was key to identifying the merger of a He-core and a CO-core white dwarf as their formation channel. ^{18}O is synthesized by the partial helium burning reaction $^{14}N(\alpha,\gamma)F^{18}(\beta^{+}\nu)^{18}O$. This reaction is efficient at temperatures of $\approx 10^8$ K (Clayton et al. 2007; Jeffery et al. 2011). At higher temperatures, ^{18}O is burnt to ^{22}Ne. These conditions can be achieved in a thin helium burning shell around the merger remnant of a He-core and a CO-core white dwarf (Clayton et al. 2007). The ^{18}O is convectively dredged up to the surface of the star within the first few hundred years after merger (Crawford et al. 2020; Munson et al. 2021; Lauer et al. 2019). The photospheric value of $^{16}O/^{18}O$ in dLHdC and RCB stars is thus set within the first hundred years and remains constant for the rest of their lifetimes ($\approx 10^{4-5}$ years). Here, we explore the properties of the merging white dwarfs that set the values of $^{16}O/^{18}O$ in the remnant supergiants. We also discuss the implications of our observations on the dLHdC-RCB connection.

5.1. Why do dLHdC and RCB stars have different $^{16}O/^{18}O$?

Studies have just begun to examine the quantities that affect $^{16}O/^{18}O$ in white dwarf merger remnants. The effects on $^{16}O/^{18}O$ of the helium burning shell temperature, convective extent of the supergiant envelope and the amount of hydrogen in the shell have been explored (Crawford et al. 2020; Munson et al. 2021). Their values in turn depend on the properties of the merging He-core and CO-core white dwarfs, such as their masses (M_{He} and M_{CO}), mass ratios and compositions. The different values of $^{16}O/^{18}O$ in dLHdC and RCB stars thus suggest a correlation between the progenitor white dwarfs' properties and dLHdC/RCB formation, which we discuss here. Note however that there are several additional factors that could contribute to the oxygen isotope ratios and remain to be modeled. A big unmodeled source of uncertainty is the effect of the initial composition of the progenitor white dwarfs and post-merger remnant on $^{16}O/^{18}O$. The correlations that we discuss below are based on current understanding and are hence preliminary. Nevertheless, they demonstrate that different properties of merging white dwarfs can result in different values of $^{16}O/^{18}O$, possibly providing a natural explanation for dLHdC versus RCB formation. Additional modeling will help establish robust relations between progenitor properties and dLHdC-RCB stars.

Crawford et al. (2020) explored the effect of the temperature of the helium burning shell (T_{He}) on $^{16}O/^{18}O$. In particular, $^{16}O/^{18}O$ drops below unity for shell temperatures in the range $T_{He} \approx 2.5 - 3.5 \times 10^8$ K. Thus, dLHdC stars could be associated with WD merger remnants that have T_{He} in this range. For shell temperatures outside this range, $^{16}O/^{18}O$ increases to RCB-like values, suggesting that RCB stars either have $T_{He} < 2.5 \times 10^8$ K or $T_{He} > 3.5 \times 10^8$ K.

From simulations of white dwarf mergers, Staff et al. (2012) found that T_{He} is inversely correlated with the mass ratio ($q = M_{He}/M_{CO}$). They derive values of $T_{He} = 3$, 2.5 and 1.5×10^8 K for $q = 0.5$, 0.6 and 0.7 respectively. The helium shell temperatures of dLHdC stars are consistent with mass ratios $0.5 < q < 0.6$. RCB stars are consistent either with $q > 0.6$ or $q < 0.5$ depending on whether they have $T_{He} < 2.5\times10^8$ K or $T_{He} > 3.5\times10^8$ K, respectively. However the Staff et al. (2012) analysis does not include an important factor – additional energy contributions from nucleosynthesis in the shell. This additional energy will increase the shell temperature, and thus the above estimates of T_{He} are likely lower limits, and the q ranges are unrealistic. No studies of temperature increase due to nucleosynthesis exist in literature.

To first order, we can estimate the temperature increase timescale assuming triple-α burning is the dominant nucleosynthetic energy source (Hansen et al. 2004). Assuming the shell parameters from Staff et al. (2012) and a 100% energy to temperature conversion, we find that the temperature of a $q = 0.7$ merger with initial $T_{He,init} = 1.5 \times 10^8$ K doubles within the first few years after merger. This time reduces to a few days for $q = 0.6$ ($T_{He,init} = 2 \times 10^8$ K) and a few minutes for $q = 0.5$

Table 2. Range of model parameters that best fit the observed spectra

Name	Class	Temperature	log(ϵ(N))	f_{dust}	$^{16}O/^{18}O$
B42 [a]	dLHDC	5000-5750	7.0	0	0.05 – 0.2
C38	dLHDC	5000-5250	9.4	0	0.05 – 0.2
B566	dLHDC	5500-6000	9.4	0	0.05 – 0.5
HD 137613	dLHDC	5000-5500	7.0-9.4	0	0.1 – 0.5
A223	dLHDC	5750 - 6000	9.4	0	0.1 – 0.5
HD 182040	dLHDC	6000	8.5-9.4	0	0.1 – 0.5
A166	dLHDC	5000 - 6000	7.0-94	0	20 – 500
HD 175893	RCB	5750	9.4	0-0.5	0.01 – 0.2
ASAS-RCB-11	RCB	5250	7.0-9.4	0-0.3	0.01 – 0.2
WX Cra	RCB	5250	9.4	0-0.1	0.05 – 0.5
EROS2-CG-RCB-6	RCB	4500-5750	7.0-9.4	0-0.8	0.2 – 5
IRAS 1813.5-2419	RCB	5750	7.0-8.5	0-0.5	0.5 – 10
S Aps [a]	RCB	5250	7.0	0-0.8	1 – 5
SV Sge [a]	RCB	5250	7.0-7.5	0-0.8	1 – 5
HV 5637	RCB	4500-5750	7.0-9.4	0-0.8	1 – 10
ES Aql [a]	RCB	5000-5250	7.0-9.4	0-0.3	2 – 10
Z Umi	RCB	5250	9.4	0.5-0.8	5 – 10
V1783 Sgr	RCB	5250	9.4	0.7-0.8	5 – 20
U Aqr	RCB	5500	9.4	0.4-0.8	5 – 20
EROS2-CG-RCB-10	RCB	4500-5750	7.0-9.4	0-0.8	5 – 50
ASAS-RCB-17	RCB	5250	7.0-8.5	0-0.2	10 – 50
NSV 11154	RCB	5250	7.0-9.4	0-0.2	10 – 50
ASAS-RCB-16	RCB	5250	7.0	0	20 – 50
ASAS-RCB-5	RCB	5500	7.0-9.4	0-0.6	50 – 500
ASAS-RCB-7	RCB	5250	7.0-9.4	0-0.4	50 – 500
ASAS-RCB-19	RCB	4500-6000	7.0-9.4	0.5-0.6	> 5
V1157 Sgr	RCB	5250	9.4	0-0.7	> 10
MACHO-401.48170.2237	RCB	4500-6000	7.0-9.4	0-0.8	> 20
WISE_J174328.50-375029.0	RCB	5250	7.0-9.4	0-0.6	> 20
ASAS-RCB-18	RCB	4750-5750	9.4	0-0.6	> 20
OGLE-GC-RCB-1	RCB	5250	7.0-9.4	0-0.4	> 50
MACHO-308.38099.66	RCB	4500-5500	7.0-9.4	0-0.8	> 50
WISE_J194218.38-203247.5	RCB	5500	9.4	0-0.1	> 50
ASAS-RCB-4	RCB	5250	7.0	0	>500
EROS2-CG-RCB-13	RCB	4500-5500	7.0-9.4	0-0.8	> 500
EROS2-CG-RCB-3	RCB	6000-6500	9.4	0-0.3	> 500
EROS2-CG-RCB-4 [b]	RCB	4500-5500	7.0-9.4	0-0.8	> 500
V517 Oph	RCB	4500-5500	7.0-9.4	0-0.8	> 500

a : The $^{12}C^{16}O$ absorption bands are possibly saturated, and the $^{16}O/^{18}O$ is likely underestimated.
b : EROS2-CG-RCB-4 shows $^{13}C^{16}O$ absorption bands.

($T_{He,init} = 3\times10^8$ K). The shell-burning temperatures for $q < 0.6$ mergers can thus exceed 4×10^8 K. RCB stars would then be consistent with low mass-ratio ($q < 0.6$) mergers and dLHdC stars would be consistent with higher mass-ratio mergers ($q > 0.7$) [4]. More detailed studies of nucleosynthetic energy production are required to determine the exact ranges of q that might form RCB and dLHdC stars

T_{He} also depends on the total mass of the white dwarf merger (Staff et al. 2018); however, the exact dependence has not been studied extensively. The Staff et al. (2012) estimates mentioned above assumed $M_{tot} \approx 0.9$ $M_\odot$. Without including nucleosynthetic energy, Staff et al. (2018) found that a $M_{tot} = 0.7$ $M_\odot$, $q = 0.5$ merger has $T_{He} < 2\times10^8$ K – lower than the estimate of 3×10^8 K for the 0.9 $M_\odot$, $q = 0.5$ merger. This suggests that lower mass mergers have lower T_{He} than higher mass mergers. Adding nucleosynthetic energy can increase T_{He} for the 0.7 $M_\odot$ merger to the dLHdC range ($2.5 - 3.5\times10^8$ K) and the 0.9 $M_\odot$ merger outside this range. dLHdC stars would then be consistent with arising from lower mass mergers than RCB stars. This would be consistent with the observation in Tisserand et al. (2021) that the population of dLHdC stars has lower luminosities than RCB stars, which they interpret as a consequence of dLHdC stars originating from lower mass mergers than RCB stars.

In addition to T_{He}, $^{16}O/^{18}O$ can also depend on the extent of the convective envelope and the mass of hydrogen in the helium burning shell (Zhang et al. 2014; Munson et al. 2021). Munson et al. explored the effect of convective overshoot factor (f) on $^{16}O/^{18}O$. They found that for $f < 0.07$, $^{16}O/^{18}O \approx 1$, but increases rapidly for $f > 0.07$. Large values of f correspond to

[4] Note that for mergers where $T_{He} > 4.5\times10^8$ K, other elemental abundances predicted by models do not agree with the observed RCB abundances (Crawford et al. 2020). This suggests that there is a lower limit on the mass-ratios of white dwarf binaries that can produce RCB/dLHdC stars.

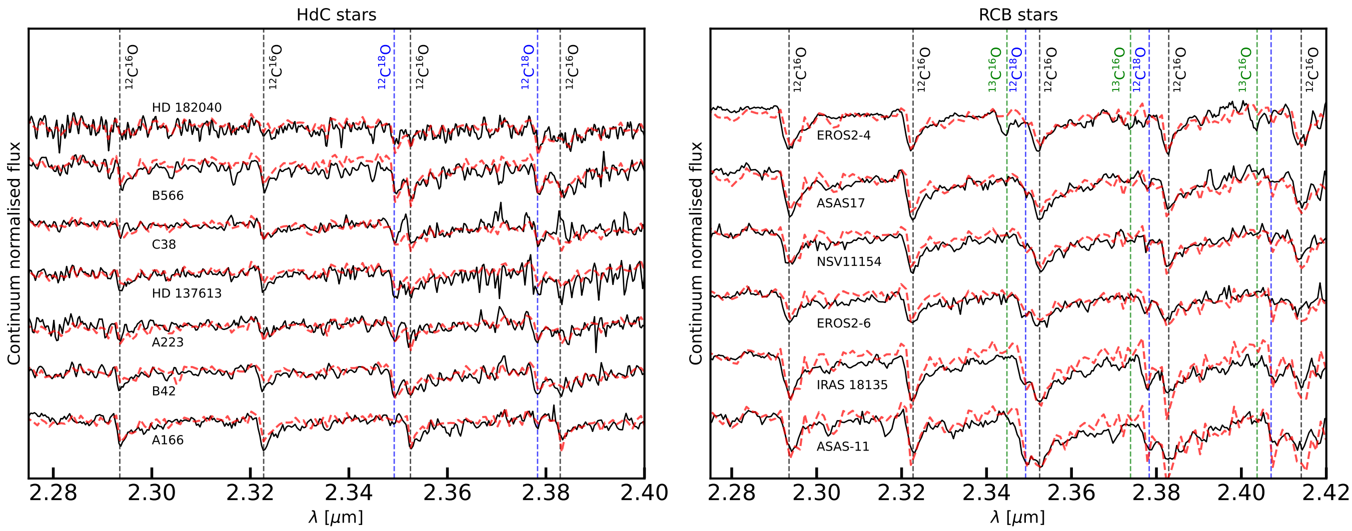

Fig. 3. Zoom-in of the $^{12}C^{16}O$ and $^{12}C^{18}O$ absorption bands of all seven dLHdC stars (left) and six representative RCB stars (right) from our sample. All dLHdC stars except A166 show strong $^{12}C^{18}O$ absorption, comparable in strength to the $^{12}C^{16}O$ absorption. The RCB stars show a range of $^{12}C^{18}O$ absorption strengths. Shown are two RCB stars where the $^{12}C^{18}O$ absorption is strongest, two where it is of intermediate strength and two where the absorption is weak. We also plot examples of synthetic spectra that fit the observed spectra as red dashed lines. Note that the RCB star EROS2-CG-RCB4 shows $^{13}C^{16}O$ absorption bands (right panel).

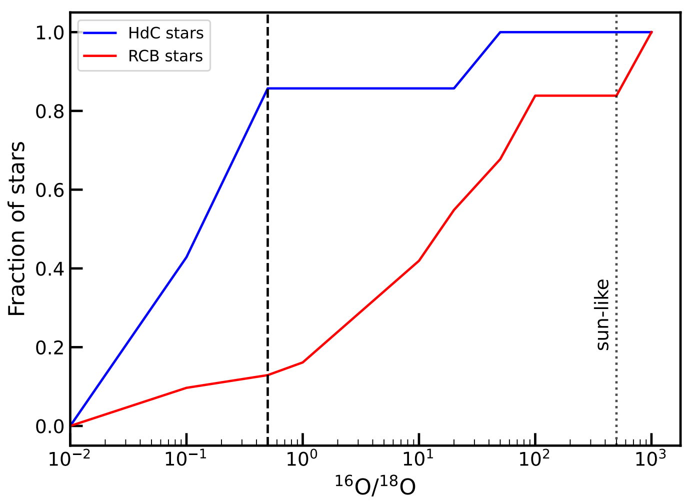

Fig. 4. Cumulative distribution plot showing the fraction of dLHdC and RCB stars that have $^{16}O/^{18}O$ below a given value. 85% (6 out of 7) dLHdC stars have $^{16}O/^{18}O < 0.5$ (black dashed line) while only $\approx 15\%$ of RCB stars (5 out of 31) are consistent with such low $^{16}O/^{18}O$ values. Most dLHdC stars have a lower $^{16}O/^{18}O$ than most RCB stars. A166 is the only dLHdC star that has $^{16}O/^{18}O > 1$. This star is an outlier amongst the newly discovered dLHdC stars, and is likely an RCB star in a low phase of dust production (see Sec. 4.1).

cases where the convective envelope extends all the way to the CO core and dredges up additional ^{16}O from the core into the envelope. The high values of $^{16}O/^{18}O$ in RCB stars could be partly explained due to such a deep convective dredge up. That will also reduce C/O in RCB stars compared to dLHdC stars. The initial conditions of a merging system that would give rise to a deep convective zone remain to be explored. Munson et al. (2021) also showed that $^{16}O/^{18}O$ increases with increasing mass of hydrogen in the helium-burning shell. The presence of hydrogen leads to a decrease of ^{18}O and increase in ^{16}O due to proton capture reactions. The source of this hydrogen is a thin hydrogen envelope around the progenitor He white dwarf (Zhang et al. 2014). The mass of the hydrogen envelope is inversely correlated with the mass of the He white dwarf (Staff et al. 2012; Driebe et al. 1998). However, a significant fraction of this hydrogen is expected to be burned during the merger. How much of the envelope hydrogen actually reaches the helium shell is not known.

In conclusion, the $^{16}O/^{18}O$ values in white dwarf merger remnants are affected by the properties of the merging white dwarfs such as their total mass, mass ratios and individual compositions. In this context, the different values of $^{16}O/^{18}O$ in dLHdC and RCB stars indicate that they are formed from distinct populations of progenitor white dwarf binary mergers.

5.2. Is there an evolutionary link between dLHdC and RCB stars?

García-Hernández et al. (2010) proposed an evolutionary link between dLHdC and RCB stars. They note that depending on the masses and compositions of the merging white dwarfs, the merger remnant will have different initial temperatures on the supergiant track. They associate dLHdC stars with the cooler parts of the supergiant track and RCB stars with hotter temperatures. In their model, depending on merger conditions the merger may first form a cold dLHdC star and eventually evolve to an RCB star, or directly form an RCB star.

Our new observations show that this picture is incorrect. First, several newly discovered dLHdC stars have higher photospheric temperatures than many RCB stars (Tisserand et al. 2021, submitted). Second, the spectra presented and analyzed here demonstrate that dLHdC stars in general have different values of $^{16}O/^{18}O$ than RCB stars (Section 4.1). As the surface abundances of dLHdC and RCB stars remain constant throughout their lifetimes (Crawford et al. 2020), it is not possible for one class to evolve into another.

Instead, we propose that whether a white dwarf merger forms a dLHdC or an RCB depends solely on the properties of the merging white dwarfs. The merger forms a dLHdC star (no significant dust formation, low $^{16}O/^{18}O$) or an RCB star (dust formation, high $^{16}O/^{18}O$) based on the mass ratios, masses and compositions of the white dwarfs. In this picture, it is still a mystery why RCB stars form large amounts of dust while dLHdC stars do not. It seems reasonable to expect that only those white dwarf mergers that are more massive than a certain threshold or have particular ranges of chemical compositions form remnants that can undergo dust formation. Future studies that more precisely identify the differences between dLHdC and RCB star progenitors could provide an answer to this question.

5.3. The overlap between dLHdC and RCB stars

An intriguing observation is the five RCB stars (classified based on their observed IR excesses and brightness declines) that show low, dLHdC-like $^{16}O/^{18}O$. These "overlap" stars may be a consequence of there being several different factors that contribute to $^{16}O/^{18}O$. For example, they could arise from typical RCB-like mass-ratio mergers but with a smaller total mass, smaller convective envelope or a smaller hydrogen content than typical. Another interesting possibility is that some dLHdC stars undergo a short-lived, dust forming phase. During this phase, these stars would be observed as dust-forming RCB-like stars with low $^{16}O/^{18}O$ - similar to the five RCB stars mentioned above. This scenario does not contradict the observation that dLHdC stars do not show significant excesses in the mid-IR WISE bands. Tisserand et al. 2021 show that the emission from a circumstellar dust shell ejected from the surface of a star shifts from the mid-IR to longer wavelengths within a few decades. Thus, even if some dLHdC stars experienced dust formation $\sim$ 10 years before their WISE observations, they would not show any excesses in the WISE bands. The dust around them would have cooled to $<$ 50 K (see Montiel et al. 2018) and would be observable only at very long wavelengths. Only one dLHdC star has been observed at far-infrared (FIR) wavelengths to date – HD 173409 which did not show any FIR excess (Montiel et al. 2018). FIR and sub-mm observations of the newly identified dLHdC stars will help confirm or rule out the presence of a cold dust shell around them.

Finally, we note that four newly discovered dLHdC stars (A166, C526, F75 and F152) show definite signs of dust formation from their mid-IR colors and light curves (see Sec. 4.5 of Tisserand et al. 2021). Of these, A166 is an outlier within the dLHdC population (see Sec. 4.2.1), has RCB-like $^{16}O/^{18}O$ and is likely an RCB star in a low dust-production phase. The three other stars are not outliers, but are too hot to sustain $^{12}C^{16}O$ and $^{12}C^{18}O$ in their photospheres so their $^{16}O/^{18}O$ cannot be constrained. Sub-mm searches for the colder circumstellar medium of these stars can determine whether they have dLHdC-like or RCB-like $^{16}O/^{18}O$ values. Additional studies of such "overlap" stars are necessary to understand the dust-formation connection between dLHdC and RCB stars.

6. Summary and way forward

^{18}O has been key to understanding the origins of the enigmatic dLHdC and RCB stars. The anomalously large ^{18}O abundance in them can be explained by invoking a He-core and a CO-core white dwarf merger model for their formation. Although there were indications that RCB and dLHdC stars have different values of $^{16}O/^{18}O$, the limited sample of dLHdC stars prevented a quantitative comparison. In this paper, we have utilized the revolutionary discovery of 27 new Galactic dLHdC stars to revisit this question.

We analyzed NIR spectra of 24 dLHdC stars together with unpublished spectra of 47 RCB stars. We derived $^{16}O/^{18}O$ ratios for 7 dLHdC and 31 RCB stars whose spectra contain the $^{12}C^{16}O$ and/or $^{12}C^{18}O$ bands. We find that six of the seven dLHdC stars have $^{16}O/^{18}O < 0.5$, while 26 of the 31 RCB stars have $^{16}O/^{18}O$ > 1. This conclusively shows that most dLHdC stars have lower $^{16}O/^{18}O$ than RCB stars. This is the only known chemical difference between these two classes of HdC stars. It remains to be seen if the lower $^{16}O/^{18}O$ is related to the lack of dust formation in dLHdC stars.

The different oxygen isotope ratios suggest that there is no evolutionary link between the class of dLHdC and RCB stars. Instead, this observation is consistent with the picture that dLHdC and RCB stars are formed from merging white dwarfs with distinct masses, mass ratios and compositions. Further theoretical studies are required to accurately determine the properties of white dwarfs that merge to form dLHdC versus RCB stars. A small number of RCB stars have uncharacteristically low, dLHdC-like $^{16}O/^{18}O$ values. This could be a consequence of multiple white dwarf properties that can affect the value of $^{16}O/^{18}O$ in the merger product, or can be explained by a short-lived dust formation phase in dLHdC stars. Theoretical models will test the former scenario, while FIR and sub-mm observations will confirm or rule out the latter. Further investigations of these "overlap" stars will shed light on the dLHdC-RCB dust formation mystery.

Future higher resolution NIR spectroscopy of the newly discovered dLHdC stars with CO bands will allow accurate determinations of their $^{16}O/^{18}O$ ratios. High resolution optical spectroscopy should allow the determination of accurate fluorine abundances in them. As fluorine is also a signature of a white dwarf merger (Pandey et al. 2007), these observations will help determine the properties of progenitors of the hot dLHdC stars that do not show CO overtone bands. High resolution spectroscopy also will potentially identify additional chemical differences between dLHdC and RCB stars and shed further light on their progenitor white dwarf populations.

Acknowledgements. We thank Bradley Munson for useful comments and discussions. PT acknowledges financial support from "Programme National de Physique Stellaire" (PNPS) of CNRS/INSU, France. MMK acknowledges the Heising-Simons foundation for support via a Scialog fellowship of the Research Corporation. MMK acknowledges generous support from the David and Lucille Packard Foundation. SA acknowledges support from the GROWTH PIRE grant 1545949. GC and CC are grateful for support from National Science Foundation Award 1814967. This research is based in part on observations for programs GN-2005B-Q-20 and GN-2011A-Q-112 obtained at the international Gemini Observatory, a program of NSF's NOIRLab, which is managed by the Association of Universities for Research in Astronomy (AURA) under a cooperative agreement with the National Science Foundation. on behalf of the Gemini Observatory partnership: the National Science Foundation (United States), National Research Council (Canada), Agencia Nacional de Investigación y Desarrollo (Chile), Ministerio de Ciencia, Tecnología e Innovación (Argentina), Ministério da Ciência, Tecnologia, Inovações e Comunicações (Brazil), and Korea Astronomy and Space Science Institute (Republic of Korea).

References

Alvarez, R., & Plez, B. 1998, A&A, 330, 1109
Asplund, M., Gustafsson, B., Lambert, D. L., & Rao, N. K. 2000, A&A, 353, 287
Bell, R. A., Eriksson, K., Gustafsson, B., & Nordlund, A. 1976, A&AS, 23, 37
Clayton, G. C. 1996, PASP, 108, 225
—. 2012, Journal of the American Association of Variable Star Observers (JAAVSO), 40, 539
Clayton, G. C., Geballe, T. R., & Bianchi, L. 2003, ApJ, 595, 412
Clayton, G. C., Geballe, T. R., Herwig, F., Fryer, C., & Asplund, M. 2007, ApJ, 662, 1220
Clayton, G. C., Herwig, F., Geballe, T. R., et al. 2005, ApJ, 623, L141

Clayton, G. C., Sugerman, B. E. K., Stanford, S. A., et al. 2011, ApJ, 743, 44
Crawford, C. L., Clayton, G. C., Munson, B., Chatzopoulos, E., & Frank, J. 2020, MNRAS, 498, 2912
Cushing, M. C., Vacca, W. D., & Rayner, J. T. 2004, PASP, 116, 362
Driebe, T., Schoenberner, D., Bloecker, T., & Herwig, F. 1998, A&A, 339, 123
Eikenberry, S. S., Elston, R., Raines, S. N., et al. 2004, in Society of Photo-Optical Instrumentation Engineers (SPIE) Conference Series, Vol. 5492, Ground-based Instrumentation for Astronomy, ed. A. F. M. Moorwood & M. Iye, 1196–1207
Elias, J. H., Rodgers, B., Joyce, R. R., et al. 2006, in Society of Photo-Optical Instrumentation Engineers (SPIE) Conference Series, Vol. 6269, Society of Photo-Optical Instrumentation Engineers (SPIE) Conference Series, ed. I. S. McLean & M. Iye, 626914
Fryer, C. L., & Diehl, S. 2008, in Astronomical Society of the Pacific Conference Series, Vol. 391, Hydrogen-Deficient Stars, ed. A. Werner & T. Rauch, 335
García-Hernández, D. A., Hinkle, K. H., Lambert, D. L., & Eriksson, K. 2009, ApJ, 696, 1733
García-Hernández, D. A., Lambert, D. L., Kameswara Rao, N., Hinkle, K. H., & Eriksson, K. 2010, ApJ, 714, 144
Geballe, T. R., Rao, N. K., & Clayton, G. C. 2009, ApJ, 698, 735
Gustafsson, B., Bell, R. A., Eriksson, K., & Nordlund, A. 1975, A&A, 500, 67
Gustafsson, B., Edvardsson, B., Eriksson, K., et al. 2008, A&A, 486, 951
Hansen, C. J., Kawaler, S. D., & Trimble, V. 2004, Stellar Energy Sources (New York, NY: Springer New York), 271–327
Herter, T. L., Henderson, C. P., Wilson, J. C., et al. 2008, in Society of Photo-Optical Instrumentation Engineers (SPIE) Conference Series, Vol. 7014, Proc. SPIE, 70140X
Jeffery, C. S., Karakas, A. I., & Saio, H. 2011, MNRAS, 414, 3599
Karambelkar, V. R., Kasliwal, M. M., Tisserand, P., et al. 2021, ApJ, 910, 132
Lauer, A., Chatzopoulos, E., Clayton, G. C., Frank, J., & Marcello, D. C. 2019, MNRAS, 488, 438
Montiel, E. J., Clayton, G. C., Sugerman, B. E. K., et al. 2018, AJ, 156, 148
Munson, B., Chatzopoulos, E., Frank, J., et al. 2021, ApJ, 911, 103
Pandey, G., Lambert, D. L., & Kameswara Rao, N. 2007, arXiv e-prints, arXiv:0712.3971
Plez, B. 2008, Physica Scripta Volume T, 133, 014003
Ramsay Howat, S. K., Todd, S., Leggett, S., et al. 2004, in Society of Photo-Optical Instrumentation Engineers (SPIE) Conference Series, Vol. 5492, Ground-based Instrumentation for Astronomy, ed. A. F. M. Moorwood & M. Iye, 1160–1171
Rayner, J. T., Toomey, D. W., Onaka, P. M., et al. 2003, PASP, 115, 362
Staff, J. E., Menon, A., Herwig, F., et al. 2012, ApJ, 757, 76
Staff, J. E., Wiggins, B., Marcello, D., et al. 2018, ApJ, 862, 74
Tisserand, P. 2012, A&A, 539, A51
Tisserand, P., Clayton, G. C., Welch, D. L., et al. 2013, A&A, 551, A77
Tisserand, P., Clayton, G. C., Bessell, M. S., et al. 2020, A&A, 635, A14
Vacca, W. D., Cushing, M. C., & Rayner, J. T. 2003, PASP, 115, 389
Webbink, R. F. 1984, ApJ, 277, 355
Zhang, J., Wang, X., Mazzali, P. A., et al. 2014, ApJ, 797, 5